

Contents

1 Literature Review	3
1.1 Overview	3
1.1.1 Faster Diagnosis	3
1.2 Traditional Methods of Machine Learning	4
1.3 State-of-the-Art	5
1.4 Related Work	8
1.4.1 CheXNet	8
1.4.2 Multi-task Learning for Chest X-ray Abnormality	9
1.4.3 Abnormality Detection and Localization in Chest X-Rays using Deep Convolutional Neural Networks	12
1.5 Analysis of Related Work	15
1.6 Medical Images	16
1.6.1 Challenges	16
1.7 Summary of Review	17
1.8 Moving Forward	17
2 Requirements Analysis	19
2.1 Deep Learning Model	19
2.1.1 Functional Requirements	19
2.1.2 Non-Functional Requirements	20
2.2 Web App for visualisation	21
2.2.1 Functional Requirements	21
2.2.2 Non-Functional Requirements	21
2.3 Methodology	22
3 Experiment Setup	23
3.1 Hardware Implementation	23
3.2 Software Implementation	24
3.3 Dataset	24

3.3.1	Dataset Preprocessing	26
3.3.2	Normalising Images	27
3.4	Evaluation Metrics-Going Beyond Accuracy	27
References		28

Chapter 1

Literature Review

This chapter is a review of the relevant literature around deep learning and how this type of machine learning has advanced in the past years . In particular, the report will discuss how deep learning can be used in the diagnosis of pathologies in chest X-rays. As well as this we will review successful projects from the past that are closely linked to this thesis.

1.1 Overview

Radiology is a branch of medicine which uses medical imaging technology to generate images so that radiologists can view structures within the human body. The types of images range from X-rays, CT scan(computed tomography scan) and ultrasounds. ([Bradley, 2008](#)). For the past few years, radiology departments in the UK have seen disruption in the National Health Service(NHS). A reoccurring issue amongst radiology departments is lack of staff to interpret scans. According to the Royal College of Radiologists, the NHS does not have enough radiologists to meet diagnostic imaging demands leaving patients at risk. ([Rimmer, 2017](#)).

1.1.1 Faster Diagnosis

One area which can augment the diagnosis of medical scans is image classification. This process of image classification involves teaching a model to learn features from images and then test on unseen images to compute accuracy. In recent times, image classification through deep learning methods has produced superhuman performance on several image-based classification tasks([Krizhevsky, Sutskever, & Hinton, 2012](#)).

1.2 Traditional Methods of Machine Learning

Before the advancements in deep learning, less sophisticated methods of image classification were employed. This method of machine learning required the crucial step of feature extraction before inputting data into a classifier. In order to visualise the process that needs to take place when using traditional methods of machine learning please refer to figure 1.1.

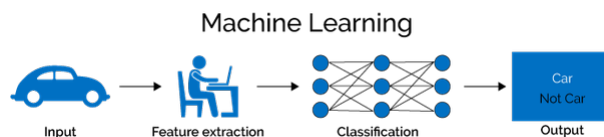


Figure 1.1: Figure showing the process of traditional image classification using feature extraction(Image taken from TowardsDataScience)

Computers see images as pixel values, and each image can be viewed as a 2D matrix of pixel values. When building a machine learning pipeline to classify an image, we need to be able to tell what is unique about each image so that the classifier shown in figure 1.1 can correctly classify. This uniqueness in an image can also be viewed as the features. Classification can then be thought of as detection of features in an image, and if features associated with a class are present in the input, we can predict if the input image is of a specific class ([Alexander, 2019](#))

In order to build a classification pipeline, the model needs to know what features it is looking for in an input image. These features it is looking for are a predefined set of features. In order to apply this rule, we can leverage human knowledge about a picture in a given domain and extract the most important features. We can then detect those manual features and use that detection to make a classification prediction ([Popescu & Sasu, 2014](#))

However, images can have lots of variation. If we want to build a robust pipeline, our model needs to be invariant to image variation, while still being sensitive to the differences in individual classifications. Manual features defined by humans can be used, but where this manual detection breaks down is in the detection task itself, and this is merely based on the fact that one class can have incredible amount of variation. This can be illustrated with the [1.2](#) provided by ([Szegedy et al., 2015](#))



Figure 1.2: Two distinct class from 1000 classes of the ImageNet database. Domain knowledge is required to distinguish between separate classes

So, how can we do better? We want a way to both extract features and detect their presence in an image automatically. This is where deep learning can be harnessed to extract features, no matter how the image is presented, automatically.

1.3 State-of-the-Art

Convolutional Neural Networks are a special kind of Multi-layered Perceptron(MLP). Like almost every other neural network they are trained with a version of back-propagation algorithm. Where they differ is in the architecture. This contrast can be viewed in figure 1.3 and figure 1.4. CNN's are designed to recognise visual patterns directly from pixel values with minimal preprocessing. They can recognise patterns with extreme variability(such as handwritten characters) and with robustness to distortions and simple geometric transformations. ([LeCun et al., 1989](#)) CNN's differ from MLP's in that they take advantage of spatial information of an image by convolving a patch of the input image with a filter weight of the same dimension. This results in a 2D matrix called a feature map. These filter weights are applied over the whole image and are iteratively refined in the training process , so that the correct features can be extracted. Different weight filter can be used to extract different features. This is achieved by passing the input across multiple convolution layers. In order to visualise this please refer to figure 1.4. From the diagrams it can be appreciated that MLP's lose all spatial information about an image by flattening every pixel and connecting these pixel values to a neuron in the hidden layer. As well as this we can see that MLP's have many more parameters in the network compared to CNN which can lead to over-fitting especially if the number of training samples is limited. ([Szegedy et al., 2015](#)) Starting with LeNet-5 , CNNS's have typically had a standard stacked structured of convolutional layers, followed by ReLU operation, max-pooling and then a fully connected layer. There are variants of this basic design in different image classification

tasks and they have all yielded respective results on classification tasks such as MNIST and CIFAR. Although, the most notable includes the ImageNet classification challenge where 1.2 million images were classified into 1000 different classes. In the past years CNN architectures have dominated this challenge and the first publication using CNN architecture was produced by Alex Krizhevsky and Geoffery Hinton in 2012([Krizhevsky et al., 2012](#)). The architecture was given the name Alex-Net and achieved a top-5 error rate of 15.3% outperforming the previous state-of-the-art, SIFT ([Lowe, 2004](#)) which achieved a 26.2% error rate using traditional methods. Since then, new CNN architectures have been published with improved results and this can be seen in the table below.

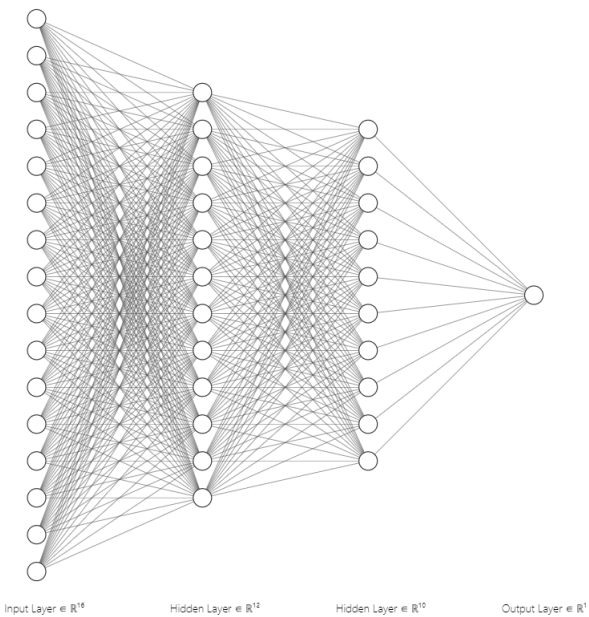


Figure 1.3: Architecture for MLP. Shows how all pixels value in image are flattened losing all spatial information(<https://alexlenail.me/NN-SVG/index.html>)

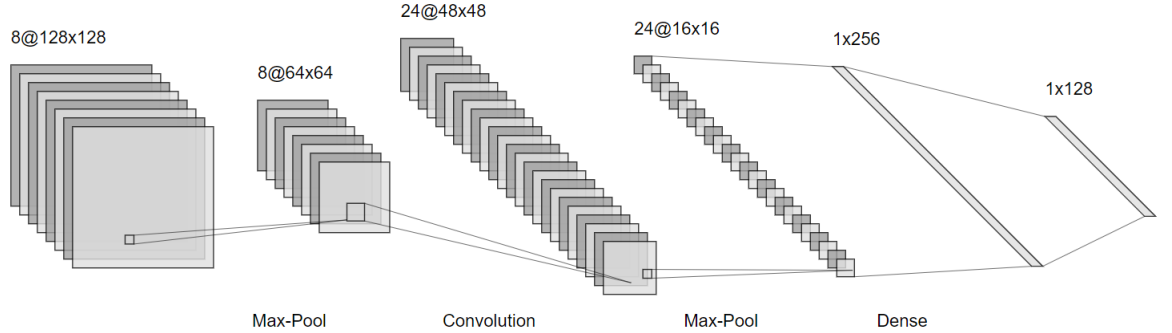


Figure 1.4: Architecture for Le-Cun CNN. Shows how spatial information is preserved as well different operations applied (<https://alexlenail.me/NN-SVG/LeNet.html>)

Model	Top-5 error rate	Number of Layers
AlexNet(2012)	15.3%	8 layers
VGG16(2014)	7.3%	19 layers
GoogleNet(2014)	6.7%	50 layers
InceptionV3(2015)	3.58%	50 layers
ResNet(2015)	3.57%	152 layers

Table 1.1: Results of different models with Human error rate at 5.1%

From the table we can see that for large datasets such as ImageNet, there is seems to be a trend developing. That is that the number of layers as well as layer size is increasing. A bigger size means that the model holds more parameters and can make it more prone to over-fitting. To address this problem, a technique developed by Google called “dropout” was developed ([Hinton, Srivastava, Krizhevsky, Sutskever, & Salakhutdinov, 2012](#))

1.4 Related Work

Many papers have been published in the domain of using deep learning for medical image analysis. This has been spurred in part due to large carefully curated labelled datasets which have led to papers showing expert-level performance on many medical image classification tasks ([Irvin et al., 2019](#)). In this section we will review work related to the thesis title.

1.4.1 CheXNet

In this project, led by Stanford ML Group, an algorithm was developed to interpret chest X-ray images and detect if Pneumonia is present while showing a heat map of the area in the image that had the highest activations ([Rajpurkar et al., 2017](#)). Example output can be see in figure 1.5

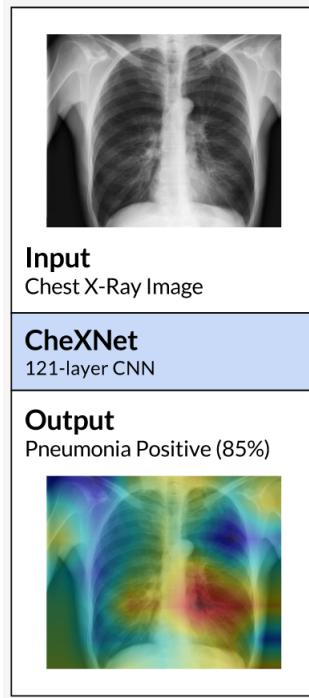


Figure 1.5: Example of CheXNet output of class label along with probability from softmax layer and heat-map

Results showed that the algorithm can detect the pathology at a level exceeding radiologists. The algorithm used a 121-layer CNN which was trained on ChestX-ray14 ([Wang et al., 2017](#)) which is currently the largest publicly available chest X-ray dataset, containing over 100,000 frontal view images and 14 different pathologies. The CNN used is based on the DenseNet architecture ([Huang, Liu, Van Der Maaten, & Weinberger,](#)

2017) but modifications were made for single output in the fully connected layer by applying a non-linearity sigmoid function, so that only Pneumonia would have a probability. Pre-trained weights were initialised from a model trained on ImageNet (Deng et al., 2009) to speed up the process of training.

1.4.1.1 Results

Precautions were put in place to make sure that patient images between training and testing sets never overlap. In order to test the accuracy of the model, 420 chest X-rays were collected and 4 practising radiologists annotated where they think the Pneumonia is present. Through the CheXNet tests it showed the algorithm exceeds average radiologist performance on the **F1 metric**. The model was comparative with expert radiologists on metrics such as **accuracy**, **sensitivity** and **specificity**. The biggest difference was in terms of speed as radiologists took around 4 hours on average to interpret the images whereas CheXNet algorithm took less than 2 minutes (Rajpurkar et al., 2017). Results from figure 1.6 present the F1 score for algorithm and average of the 4 clinicians.

	F1 Score (95% CI)
Radiologist 1	0.383 (0.309, 0.453)
Radiologist 2	0.356 (0.282, 0.428)
Radiologist 3	0.365 (0.291, 0.435)
Radiologist 4	0.442 (0.390, 0.492)
Radiologist Avg.	0.387 (0.330, 0.442)
CheXNet	0.435 (0.387, 0.481)

Figure 1.6: F1 Score for CheXNet and average F1 score for 4 radiologists

1.4.2 Multi-task Learning for Chest X-ray Abnormality

In this paper, researchers built a model trained on 297,541 chest X-rays. The system is based on a novel multi-task deep learning architecture that in addition to classifying and showing a heat-map of the abnormalities also supports the segmentation of the lungs and heart (Guendel et al., 2019). The research demonstrated that by training the model concurrently on these tasks, one can increase the classification performance. This research produced state of the art performance of 0.883 AUC on average across 12 different abnormalities. ChestX-Ray 14 (Wang et al., 2017) and PLCO datasets were combined to increase the amount of variability of images and this also showed increase in performance.

As mentioned before techniques were applied to increase accuracy. One of the methods

employed was to normalise the images. A challenge in processing chest radiographs is that there can be large variabilities in the appearance of the image and this is due to the acquisition source, radiation dose ([Guendel et al., 2019](#)). The paper proposes to dynamically window each image by adjusting the brightness and contrast via a linear transformation of the image intensities. Example of output is shown in figure [1.7](#)



Figure 1.7: We can see that certain parts of the X-ray become more visible hence making abnormalities more clear for the model

In addition , the paper also harnesses spatial knowledge related to individual pathologies as well as underlying structure i.e the heart and lungs which can be exploited to increase classification performance. The paper proposes that once can focus the learning task to the heart and lung region as information outside of these regions may be regarded as irrelevant for the diagnosis of heart/lung abnormalities.

In order to achieve this segmentation, a DenseNet model shown in figure [1.8](#) ([Huang et al., 2017](#)) has been used and figure [1.9](#) presents the architecture as well as an example showing the segmentation technique. Another technique that was used to take advantage of spatial information was the use of several approximate spatial labels provided in the PLCO dataset. For five abnormalities(Nodule,Mass,Infiltrate,Atelectasis,Hilar Abnormality) there are rough location information available to help the model locate where the abnormality is usually located.

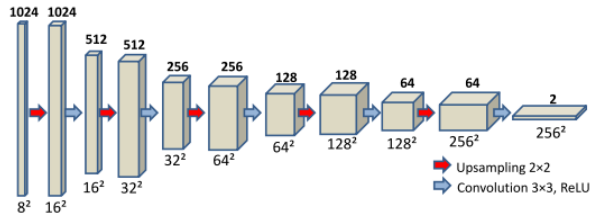


Figure 1.8: Architecture for DenseNet

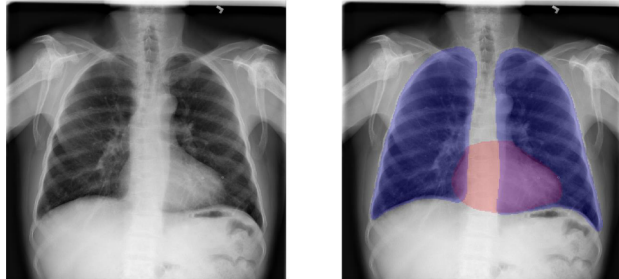


Figure 1.9: Distinct segmentation of lungs and heart

1.4.2.1 Results

For this paper, different experiments were undertaken to show the performance of the model. As a baseline, performance was measured by only training the classification part on the PLCO dataset. The test was evaluated with an average **AUC** score across 12 abnormalities of **0.859**.

Results also showed improved classification scores when the network was additionally trained to generate lung and heart segmentation masks (as shown in figure 1.10). Performance increased to 0.866 on average across the abnormalities.

As mentioned another technique was to use spatial knowledge and the impact of this showed an average improvement of 0.011

This paper also used 2 datasets and by combining both, the average AUC score reaches 0.870. This increase in score is due to more variability in the learning process. As well as this the normalisation technique previously shown in figure 1.7 was applied when training the model and this had a 2 fold benefit. The first was that the training process was reduced on average 2-3 times. The researchers hypothesised that this is due to the images being more aligned in terms of brightness and contrast. Another reason was due to the generalisation of the model parameters and this lead to a performance gain of 0.876.

Finally, the researchers upscaled the input image size to 512 in each dimension and adjusted the DenseNet layer to take in 16x16 patch size at each layer. This final network architecture change also added all of the previous techniques mentioned before. The following image shows the results obtained across all techniques and finally the result of combining all the techniques which produces a state-of-the-art performance of **0.883**

Dim. Size	256 × 256	256 × 256	256 × 256	256 × 256	256 × 256	512 × 512
Data	PLCO	PLCO	PLCO	PLCO+NIH	PLCO+NIH	PLCO+NIH
Features	-	Seg.	Loc.	Loc.	Loc.+Norm.	Loc.+Norm.+Seg
Nodule	0.810	0.815	0.830	0.832	0.831	0.881
Mass	0.829	0.839	0.840	0.867	0.869	0.884
Granuloma	0.884	0.886	0.887	0.887	0.893	0.912
Infiltrate	0.865	0.863	0.864	0.877	0.882	0.891
Scaring	0.841	0.842	0.843	0.850	0.848	0.861
Fibrosis	0.870	0.875	0.863	0.875	0.871	0.884
Bone/Soft Tissue Lesion	0.841	0.846	0.834	0.840	0.850	0.848
Cardiac Abnormality	0.926	0.928	0.922	0.923	0.927	0.926
COPD	0.882	0.883	0.877	0.880	0.882	0.874
Effusion	0.909	0.938	0.927	0.932	0.949	0.939
Atelectasis	0.849	0.858	0.858	0.867	0.855	0.832
Hilar Abnormality	0.796	0.815	0.812	0.815	0.850	0.859
Mean (Location Labels)	0.830	0.838	0.841	0.852	0.857	0.869
Mean	0.859	0.866	0.863	0.870	0.876	0.883

Figure 1.10: Results showing increasing mean AUC score

1.4.3 Abnormality Detection and Localization in Chest X-Rays using Deep Convolutional Neural Networks

For this paper, researchers conducted experiments on three datasets. From the datasets, researchers explored the performance of various deep CNN's for detection of heart disease from chest X-rays. Researchers used binary classification on diseases such as Cardiomegaly against normal images ([Islam, Aowal, Minhaz, & Ashraf, 2017](#)). The paper explores several CNN models such as AlexNet, VGG-Net and ResNet. These models have different layers and typically achieve higher accuracy as layers increase as noted in State-of-the-Art section.

Another part of the research, similar to previous papers reviewed was to produce a heat-map showing which areas of the X-ray the model has the highest activation on. This paper used the sensitivity of softmax scores of occlusion on a certain region in the chest X-ray to find which region in the image is responsible for the classification decision.

1.4.3.1 Results

The first experiment used single model CNN's on the Indiana dataset, and from the tests, it was shown that deeper models like VGG-19, ResNet improve the accuracy significantly. It was found that Cardiomegaly detection improves 6% compared to using shallower models like AlexNet. Although results showed high specificity for ResNet-101 and high sensitivity for VGG-16, the VGG-19 gave the highest AUC score of 0.94. This at least 1% higher AUC for other models. As well as this, dropout was used, which increased performance on the shallower networks but degraded deeper ones. For all experiments, it was noted that extracting features from earlier layers lead to improved accuracy of 2-4%. It was concluded that shallower networks were better for detecting smaller objects, and as an example, it was found that shallower layers from ResNet-15 trained on Cardiomegaly had better performance than later layers across different

metrics. figure 1.11 shows a more in depth picture of findings.

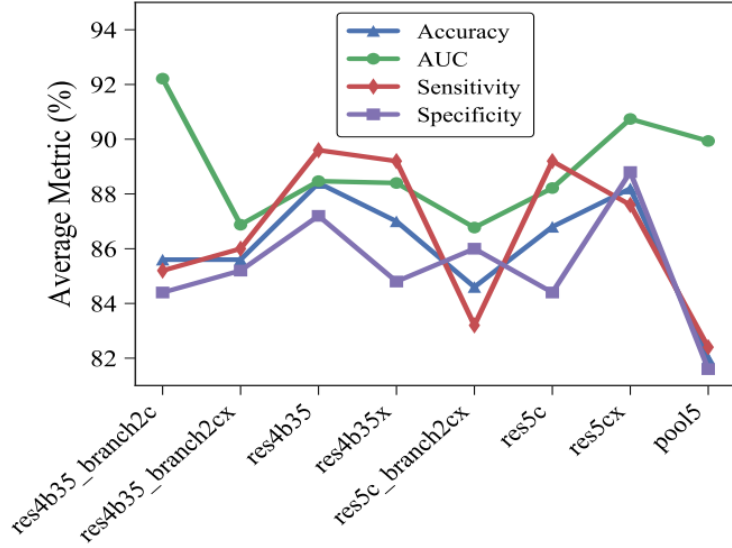


Figure 1.11: Researchers showed that shallower layers in models had a higher accuracy on Cardiomegaly detection compared to deep layers

Another fascinating result was on the localisation of Cardiomegaly shown in the image below. It can be observed that from the figure 1.13, the model has higher activations from the heart region, which is expected as Cardiomegaly concerns abnormal enlargement of the heart. What was revealing was that other than an enlarged heart for a patient with Cardiomegaly, there is not much difference in features between a normal image and an image classified as Cardiomegaly. But the model can still differentiate between a normal heart which is enlarged due to age or physical attributes of the patient.



Figure 1.12: Occlusion sensitivity used to create heap map of region where it thinks Cardiomegaly exists

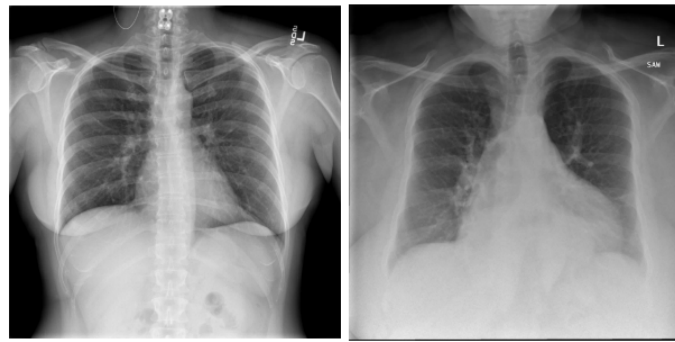


Figure 1.13: Example of normal heart on the left and Cardiomegaly diagnosed heart on the right

Finally, another point raised in the paper was the model used for localisation of cardiomegaly were counter-intuitive to traditional methods of cardiomegaly diagnosis, which consider the relative size of heart and lung. But, most of the signals contributing to the softmax score come from the heart alone indicating features in the shape of the heart and its surrounding region alone help in detection of the pathology and perhaps the lung and relative size to the heart are less critical in the diagnosis for the model.

1.5 Analysis of Related Work

In light of reviewing the related work, we can see a wide array of methods have been applied to produce several State-of-the-Art results on pathologies such as Pneumonia, Lung Nodules and Cardiomegaly. The paper from Stanford ML Group was one of the first to be tested on such a large scale dataset and made a mark in the application of deep learning on X-rays. Results from this paper show a 121-layered network produce results comparable to expert radiologists by using an architecture similar to that of DenseNet with some tweaks. As stated the ChexNet model has a higher F1 score than the average F1 score for four practising radiologists. After the success of ChexNet, more papers were released in the same domain trying to improve on accuracy metrics. The article discussed in section 1.4.2 uses more advanced features to locate the pathology more accurately. Given these additional features, it allows for the model to disregard certain regions of the images hence reducing noise in training process. From the results presented. It shows a clear improvement in accuracy across different pathologies once these features are introduced to the model. Lastly, the paper from X demonstrates a clear difference of performance on known CNN architectures. In section X, it showed that deeper layers led to better performance on the ImageNet classification task. However contrary to most image classification tasks, paper shown in section 1.4.3 shows how even though we see a better accuracy on deeper models, we see a higher AUC score for models like VGG-19 compared to ResNet-101, which has more layers, and this was due to earlier layers being better at detecting smaller objects. We also see the use of an ensemble of models to increase accuracy, which was something that was not experimented with in the previous papers reviewed. As well as this, we see a model trained on Cardiomegaly questioning the current ways of detecting this pathology such that it disregards traditional methods of looking at the relative size of the lung and heart in comparison. Lastly, from the three papers reviewed, we have seen the constant evolution which has allowed for more sophisticated methods of pathology detection and perhaps a combination of techniques in the future can increase detection amongst heart and lung pathologies.

1.6 Medical Images

As mentioned in the Overview section, radiology departments in the UK have struggled to meet imaging diagnostic demands. The survey published by the Royal College of Radiology reported 97% of radiology departments were unable to do so within their working hours. As mentioned in the paper, “It points to an insufficient number of radiologists to meet the increasing demand for imaging and diagnostic services”. According to the report it cited that radiology has the second lowest proportion of trainees to consultants: 26 trainees to every 74 consultants. This is compared to an average in all specialities of 40 trainees for every 60 consultants. The report also cites that there was a particular workforce shortage prominent in Scotland, where the consultant workforce grew by 7% from 2010 to 2016 but demand for CT,MRI scans increased by 10%. One of the profound impacts of such shortage is the risk to patient care as well as economical effects. The NHS paid nearly £88m in 2016 for backlogs of radiology examinations to cover backlogs of radiology examinations to be reported. To cover these backlogs 92% of radiology departments paid staff overtime, 78% outsourced to private companies and 52% employed ad hoc locums. This amount could have paid for at least 1028 full time radiology consultants.([Rimmer, 2017](#))

Given this what has been done to augment the analysis of medical images in the NHS and reduce extreme workload and large expenses ? One particular software which has bee used in the clinical setting is Computer Aided Diagnosis(CAD). CAD is technology which is designed to decrease observational oversights and false negative rates for physicians interpreting medical images such as mammographies ([Castellino, 2005](#)). According Dr. Paul Chang, the reason this type of software did not receive as much attention, compared to the possibility of using deep learning, was that it used traditional methods of machine learning. (*Video from RSNA 2018: Dr. Paul Chang on AI and radiology*, n.d.)

1.6.1 Challenges

There many challenges associated when applying new technologies in a clinical setting. Medical images are very large and complicated and for most of the image classification tasks in the ImageNet example , distinct features or pixels can be learned by a model. Dr. Matthew Lungren , radiologist at Stanford Medical Center, mentioned how most of the pixels in a chest X-Ray from a healthy person who happens to have lunge cancer , will tell you that the image is of a healthy person. But there is only a small proportion of the image which indicates the finding of lung cancer fo the classifier. Dr Lungren also noticed how medical images may have, what is known as artefacts or tokens in the image. Doctors are able to deal with context when looking at an image , but

such artefacts or tokens may lead to a model making a decision with higher degree of confidence but in actual fact the classification is incorrect ([DrMatthew, 2018](#))

1.7 Summary of Review

From the review, it is quite evident that with the ever-growing concern in the NHS of a shortage of radiologists ([Rimmer, 2017](#)), solutions need to be found in order to solve the issue of increased backlogs. Image classification, as mentioned, can provide augmentation of diagnosis of X-rays. Great leaps and bounds have been made in the field of deep learning and particularly well known CNN architectures show performance exceeding that of human intelligence in the case of ImageNet challenge ([Krizhevsky et al., 2012](#)s). As well as this more sophisticated example of applying deep CNN's to medical images has shown outstanding results on pathologies such as Pneumonia and Cardiomegaly ([Rajpurkar et al., 2017](#)). This problem of diagnosing X-rays also comes with its challenges which have been outlined in the challenges section. Other hurdles must be kept in mind for implementation purposes, and these include making sure that pixel values are not lost. Given the nature of X-rays, pixel loss can lead to pathologies being removed from an image such as lung nodules and according to the Royal College of Radiologists certain rules need to be adhered to so that images do not lose quality when it comes to diagnosing them. Lastly, when training a model on medical images, the dataset chosen needs to be balanced in class labels. As well as this one of the big obstacles is lack of datasets of reliable labelling of datasets as noise in class labels can lead to reduced performance.

1.8 Moving Forward

In this section, we will conclude how the rest of this paper will be implemented and how the proposed problem in the introduction will be approached. From the findings above the aim is to apply one of the well known CNN architectures to build an accurate image classification pipeline on predicting the presence of Pneumonia in chest X-rays. In order to train the model, a carefully curated dataset must be chosen. The dataset that will be used in this thesis comes from a public dataset carefully curated by Stanford ML Group called CheXPert. This dataset was created to solve three problems which include enough instances, strong reference standards and provide human performance metrics for comparison. It consists of 224,316 chest X-rays, and one of the main obstacles in the development of these datasets is the lack of strong radiologist-annotated ground truth. The objectives is to build an accurate model which can predict and localise the Pneumonia with techniques such as occlusion. Another objective would be to build an interface which allows the entry of a chest X-ray and a predicted class label will be

given back as well as a heat-map indicating which parts of the image had the highest activation. Lastly, if results from the initial pipeline show high accuracy, specificity, sensitivity and AUC, then the model could be extended to classify more than one pathology contained in the dataset.

Chapter 2

Requirements Analysis

In order to answer the question proposed in the literature review, several objectives must be met. As this project cover two stages: Application of deep learning model on medical images and visualisation, this requirements analysis is split up into two sections: first section relating to requirement analysis of the implementation of deep learning model and the second being visualisation.

These requirements have been gathered based on the MoSCoW rule, which prioritises different requirements by stating the project must, should or could achieve the detailed requirements by the end of the implementation stage. A requirement that the project "must" achieve has the highest priority, where if this requirement is not met, the developed product will not be fit for purpose. The ones that "should" be completed are next in the priority hierarchy, whereby the project will still be functional without them, but their addition to the project would improve the end product. The requirements that "could" be completed are those that are not necessary to the overall functionality. However, these would benefit the project.

2.1 Deep Learning Model

2.1.1 Functional Requirements

2.1.1.1 Dataset

Must pre-process images from the dataset. Since input into the neural network, used in the implementation phase, requires pixel values, every image will need to be converted to its respected pixel value. Moreover, any resizing of the images will also need to be done as input to the neural net needs to be of a specific shape. Hence, this needs to be investigated in the implementation stage.

2.1.1.2 Convolutional Neural Network

Must build a model using image classification algorithms like CNN.

2.1.1.3 Improve Performance of model

Must look into ways of tweaking model parameters, and evaluating the results of these improvements, as per the ones described in the literature review.

2.1.1.4 Comparison of different algorithms

A report showing a comparison of different algorithm employed to build a model and predict could be created depending on the time.

2.1.1.5 Extending classification

The model's architecture could be further extended to diagnose more than one pathology.

2.1.2 Non-Functional Requirements

2.1.2.1 Programming Language and Libraries

Must use Python for rapid development and prototyping of CNN model via libraries such as Keras and sci-kit learn for visualisation and explanation of results.

2.1.2.2 Proof of Concept

Must be fully functional by the proof of concept stage

2.1.2.3 Anonymised Date

Must use anonymised patient data from publicly available datasets in order to conform to GDPR rule.

2.1.2.4 Accuracy

Model should diagnose images with an acceptable accuracy rate

2.2 Web App for visualisation

2.2.1 Functional Requirements

2.2.1.1 Visualisation

If the model evaluation shows promising performance, visualisation and explainability of results must be used in the form of a web application:

- Must show a classification probability to the user when a chest X-ray is tested on the deployed model
- Should show a localisation of where the model believes the Pneumonia is present in the X-ray.

2.2.1.2 User Input

User must be allowed to upload an image through the interface and get back results from the image being tested on the model.

2.2.2 Non-Functional Requirements

2.2.2.1 Programming Language and Libraries

Must use Javascript,HTML,CSS and cloud services for web application development:

- Should use Amazon Web Services(AWS) Sage Machine and AWS Lambda to deploy trained and tested model. The model should be accessed via the deployed RESTful API

2.2.2.2 Completion Date

Must be completed by the project demonstration day or could be operational by proof of concept deadline

2.2.2.3 Compatibility

Should be compatible with all major web browsers

2.2.2.4 Image quality

Must not reduce image quality when passing image to cloud service where the model has been deployed upon

2.3 Methodology

The requirements in the previous section will be delivered in an agile manner. Using an agile approach consists of implementing the model, testing it against the test set, evaluating and reporting on the results of the performance. This process will be iterative until satisfactory results from the model are achieved, then leading to the deployment of the model onto a cloud service. The image shown in [2.1](#), demonstrates the steps that will be taken to build a model that can accurately detect the presence of Pneumonia in chest X-rays.

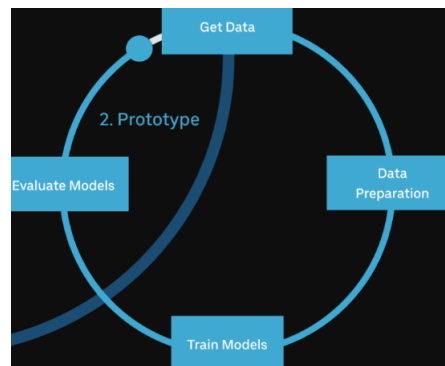


Figure 2.1: Iterative process of building deep learning model

Chapter 3

Experiment Setup

Before moving onto explaining process of applying the machine learning models for this paper, the following chapters explains the experimental setup that took place before starting the experiments. In this section the hardware and software setup is discussed. As well as this a general overview of the dataset that is used for the experiments is discussed and more importantly the preprocessing that had to occur before running experiments. Lastly evaluation metrics will be discussed so that experiments in the later chapters can be analysed against metrics that determine the success or failure of an experiment

3.1 Hardware Implementation

A computer system with the specifications show in Table 3.1 has been used to carry out the experiments in this paper. Through the help of Robert Gordon Universities Research Hub for Data Science, this project used the Research Hub's Nvidia DGX-1 machine to accelerate the experiments carried out in this paper.

Table 3.1: Computer System Specification

Operating System	Ubuntu 18.04 Linux Host OS
CPU	2x Intel Xeon E5-2698 v3 (16 core, Haswell-EP)
System Memory	512GB DDR4-2133 (LRDIMM)
GPU	8x NVIDIA Tesla P100 (3584 CUDA Cores)
GPU Memory	128GB HBM2 (8x 16GB)

3.2 Software Implementation

The setup for the experiments in this paper involves the use of **Python 3**. The solution heavily relies on **Keras**, which is an open-source neural network library written in python and is capable of running on top of **TensorFlow** as its back-end. Keras is designed to enable fast experimentation with deep neural networks and contains the basic building blocks to build one such as adding layers, objective functions, activation functions and optimisers. Moreover, Keras through the use of TensorFlow allows for the use of distributed training of deep learning models on multiple Graphics Processing Units - GPUs. This is further achieved by using CUDA, which is a parallel computing platform and Application Programming Interface(API) created by Nvidia. The CUDA platform is a software layer that gives direct access to the GPU allowing for highly parallel manipulation of large blocks of data.

3.3 Dataset

The dataset that will be used for training and testing of the learning algorithm has been taken from a public repository ([K. M. Kermany Daniel;Zhang, 2018](#)). The dataset includes X-ray images of both normal patients and patients with pneumonia infected lungs. Based on the information given by the authors that published the dataset, for use in the paper titled “Identifying Medical Diagnoses and Treatable Diseases by Image-Based Deep Learning” ([D. S. Kermany et al., 2018](#)), the data has been obtained from the Chest X-ray images selected from a respective cohort of pediatric patients aged from one to five years old from Guangzhou Women and Children’s Medical Center.

The dataset comes with two folders which include training and validation. Each folder contains subfolders for each type of classification, normal and pneumonia. The training folder contains 5218 images split into 1342 normal images and 3876 pneumonia images. The validation folder contains 624 images split into 234 normal images and 390 pneumonia images. Figures [3.1](#) and [3.2](#) help to visualise the distribution of the training and testing set respectively. The distribution of both training and testing are important to notice as this will be an important consideration when evaluating the model performance.

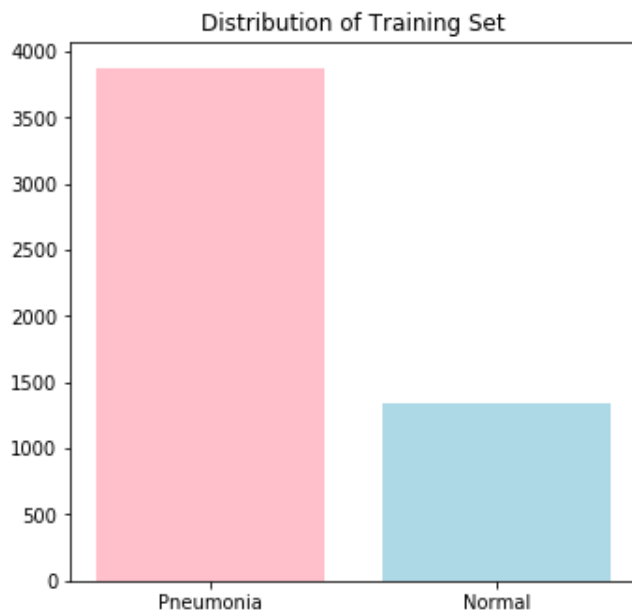


Figure 3.1: Class Distribution of Training Set

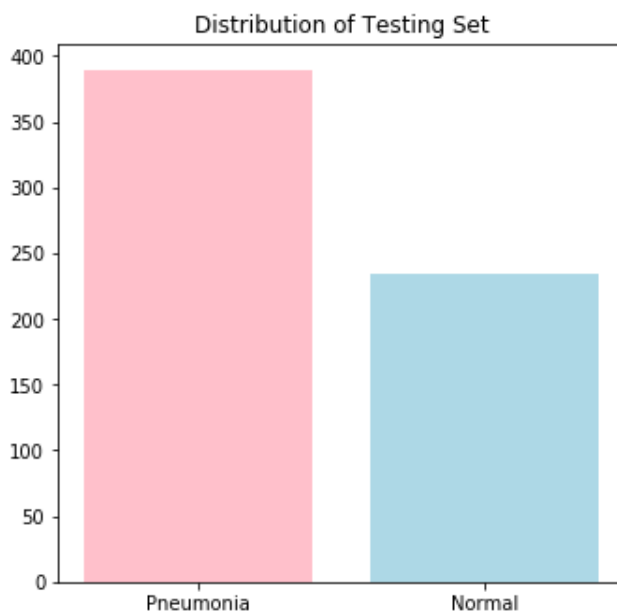


Figure 3.2: Class Distribution of Testing Set

In order to visualise the images used to train the learning algorithm , figure 3.3 and 3.4 shows an example of both a normal patient and a patient suffering from pneumonia. As might be visible in figure 3.3, a healthy X-ray would normally be clearer and the general area of the chest is more visible compared to cases where pneumonia is present as shown

in figure 3.4. It is essential to mention that the onset of pneumonia in patients can differ depending on the severity. As such, there may only be a few pixels that denote the presence of pneumonia which makes the problem of detecting the infection a challenge.

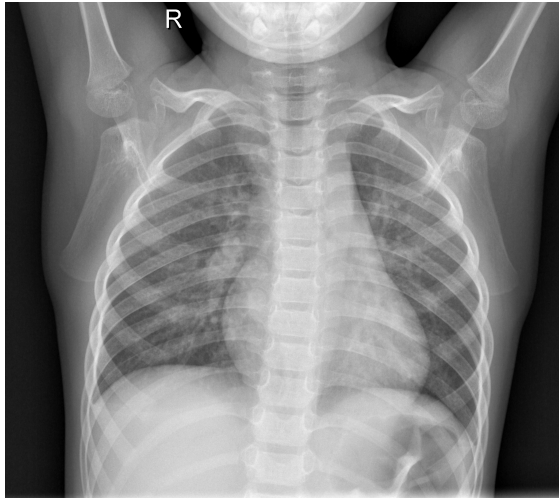


Figure 3.3: Normal Chest X-ray

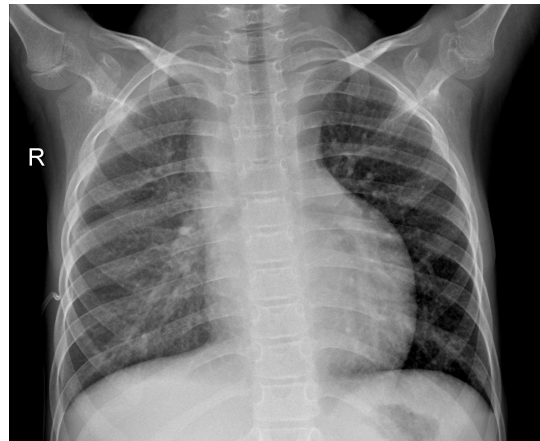


Figure 3.4: Pneumonia Chest X-ray

3.3.1 Dataset Preprocessing

During exploration of the dataset it was shown that the X-ray images provided were of different sizes. This most likely due to different X-ray imaging machines used during collection of the dataset. Before applying the learning algorithm on the X-ray images we needed to make sure that each input image was of the same dimension. This is due to the way a CNN is configured via libraries like Keras, where the size of the input layer is constant. At first, all images were resized from their original size to 250 x 250. However, due to guidance, later experiments used a size of 256 x 256.

3.3.2 Normalising Images

Data normalisation is an important step which ensures each pixel value for an image has a similar data distribution. This makes convergence faster while training a neural network. Although non-normalised data can be presented to the neural network, this can result in challenges during training, such as slower training of the model.

As discussed in section 1.3 “State of the Art”, neural networks process inputs using small weight values which are multiplied by the input value. If these inputs are on a large unsigned integer scale, like pixel values, this may disrupt or slow down convergence of the training process. A pixel value of 0(white) compared to 255(black) are both equally as important but the 255 value will have a greater effect on the final prediction. This large value could cause the output to be wrong and lead to the training process taking longer.

For the purposes of this paper, data normalisation is applied by dividing each pixel value by 255. As a result all inputs to the model have a range between 0 and 1.

To better understand the stages of normalisation, figure 3.5 shows the steps taken to normalise each image.¹

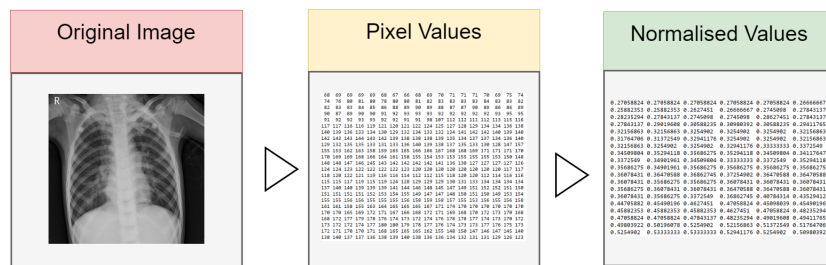


Figure 3.5: Stages of the Preprocessing and Normalisation

3.4 Going Beyond Accuracy

¹Python Notebook:Preprocessing

References

- Alexander, A. (2019). *Mit 6.s191: Convolutional neural networks*. Retrieved from <https://youtu.be/H-HVZJ7kGI0?t=6>
- Bradley, W. G. (2008). History of medical imaging. *Proceedings of the American Philosophical Society*, 152(3), 349–361.
- Castellino, R. A. (2005). Computer aided detection (cad): an overview. *Cancer Imaging*, 5(1), 17.
- Deng, J., Dong, W., Socher, R., Li, L.-J., Li, K., & Fei-Fei, L. (2009). Imagenet: A large-scale hierarchical image database. In *2009 ieee conference on computer vision and pattern recognition* (pp. 248–255).
- DrMatthew, L. (2018). *Ai in radiology at stanford: Rise of the machines*. Retrieved from <https://youtu.be/Gigd1rkZTSE>
- Guendel, S., Ghesu, F. C., Grbic, S., Gibson, E., Georgescu, B., Maier, A., & Comaniciu, D. (2019). Multi-task learning for chest x-ray abnormality classification on noisy labels. *arXiv preprint arXiv:1905.06362*.
- Hinton, G. E., Srivastava, N., Krizhevsky, A., Sutskever, I., & Salakhutdinov, R. R. (2012). Improving neural networks by preventing co-adaptation of feature detectors. *arXiv preprint arXiv:1207.0580*.
- Huang, G., Liu, Z., Van Der Maaten, L., & Weinberger, K. Q. (2017). Densely connected convolutional networks. In *Proceedings of the ieee conference on computer vision and pattern recognition* (pp. 4700–4708).
- Irvin, J., Rajpurkar, P., Ko, M., Yu, Y., Ciurea-Ilcus, S., Chute, C., ... others (2019). Chexpert: A large chest radiograph dataset with uncertainty labels and expert comparison. *arXiv preprint arXiv:1901.07031*.
- Islam, M. T., Aowal, M. A., Minhaz, A. T., & Ashraf, K. (2017). Abnormality detection and localization in chest x-rays using deep convolutional neural networks. *arXiv preprint arXiv:1705.09850*.
- Kermany, D. S., Goldbaum, M., Cai, W., Valentim, C. C., Liang, H., Baxter, S. L., ... others (2018). Identifying medical diagnoses and treatable diseases by image-based deep learning. *Cell*, 172(5), 1122–1131.

- Kermany, K. M., Daniel;Zhang. (2018). *Labelled optical coherence tomography(oct) and chest x-ray images for classification*. Retrieved from <http://dx.doi.org/10.17632/rscbjbr9sj.2>
- Krizhevsky, A., Sutskever, I., & Hinton, G. E. (2012). Imagenet classification with deep convolutional neural networks. In *Advances in neural information processing systems* (pp. 1097–1105).
- LeCun, Y., Boser, B., Denker, J. S., Henderson, D., Howard, R. E., Hubbard, W., & Jackel, L. D. (1989). Backpropagation applied to handwritten zip code recognition. *Neural computation*, 1(4), 541–551.
- Lowe, D. G. (2004). Distinctive image features from scale-invariant keypoints. *International journal of computer vision*, 60(2), 91–110.
- Popescu, M. C., & Sasu, L. M. (2014). Feature extraction, feature selection and machine learning for image classification: A case study. In *2014 international conference on optimization of electrical and electronic equipment (optim)* (pp. 968–973).
- Rajpurkar, P., Irvin, J., Zhu, K., Yang, B., Mehta, H., Duan, T., ... others (2017). Chexnet: Radiologist-level pneumonia detection on chest x-rays with deep learning. *arXiv preprint arXiv:1711.05225*.
- Rimmer, A. (2017). Radiologist shortage leaves patient care at risk, warns royal college. *Bmj*, 359, j4683.
- Szegedy, C., Liu, W., Jia, Y., Sermanet, P., Reed, S., Anguelov, D., ... Rabinovich, A. (2015). Going deeper with convolutions. In *Proceedings of the ieee conference on computer vision and pattern recognition* (pp. 1–9).
- Video from rsna 2018: Dr. paul chang on ai and radiology.* (n.d.). Retrieved from <https://youtu.be/o2-CrrrtuJI?t=300>
- Wang, X., Peng, Y., Lu, L., Lu, Z., Bagheri, M., & Summers, R. M. (2017). Chestx-ray8: Hospital-scale chest x-ray database and benchmarks on weakly-supervised classification and localization of common thorax diseases. In *Proceedings of the ieee conference on computer vision and pattern recognition* (pp. 2097–2106).